Learning by Demonstration for Planning Activities of Daily Living in Rehabilitation and Assistive Robotics

Clemente Lauretti, Francesca Cordella, Eugenio Guglielmelli, and Loredana Zollo

***Abstract*—This letter presents a motion planning system for robotic devices to be adopted in assistive or rehabilitation scenarios. The proposed system is grounded on a learning by demonstration approach based on dynamic movement primitives (DMP) and presents a high level of generalization allowing the user to perform activities of daily living. The proposed approach has been experimentally validated on a robotic arm (i.e., the Kuka LWR4+) attached to a human subject wrist. Two experimental sessions have been carried out in order to: 1) evaluate the differences between our approach and the one proposed in "Dynamical movement primitives: Learning attractor models for motor behaviors" (A. J. Ijspeert *et al.*, *Neural Comput.*, 2013) in terms of reconstruction error between the demonstrated trajectory and the learned one, and in terms of memory size required to record the database of DMP parameters; and 2) measure the generalization level of the proposed system with respect to the variation of the object positions by evaluating the success rate of the task execution. The experimental results demonstrate that the proposed approach allows 1) reproducing the user's personal motion style with high accuracy and 2) efficiently generalizing with respect to the change of object position. Furthermore, a significant reduction of memory allocation for the database can be achieved, with a consequent significant computational time saving.**

***Index Terms*—Learning from demonstration, motion and path planning, task planning.**

I. Introduction

In THE recent years, the adoption of robotic devices in rehabilitation and assistive field is widely increased for a number of reasons, e.g: they can assure a high repeatability of movements and intensity of treatment, an active role of the patients and an enhancement of their level of independence and social participation. Robot motion planning plays a paramount role in the interaction between user and assistive technology, especially for the execution of Activities of Daily Living (ADLs), which are fundamentals for a social and professional reintegration.

Manuscript received September 10, 2016; accepted January 23, 2017. Date of publication February 15, 2017; date of current version March 10, 2017. This letter was recommended for publication by Associate Editor J. Veneman and Editor K. Masamune upon evaluation of the reviewers' comments. This work was supported in part by the European Project H2020/AIDE: Multimodal and Natural computer interaction Adaptive Multimodal Interfaces to Assist Disabled People in Daily Activities (CUP J42I15000030006) and in part by the Italian Institute for Labour Accidents (INAIL) with PPR 2 project (CUP: E58C13000990001).

The authors are with the Unit of Biomedical Robotics and Biomicrosystems, Department of Engineering, Università Campus Bio-Medico, 00128 Rome, Italy (e-mail: c.lauretti@unicampus.it; f.cordella@unicampus.it; e.guglielmelli@unicampus.it; l.zollo@unicampus.it).

Color versions of one or more of the figures in this letter are available online at http://ieeexplore.ieee.org.

Digital Object Identifier 10.1109/LRA.2017.2669369

The use of patient-tailored planning strategies, compatible with human motor control strategies and able to replicate the user's personal motion style, can enable a more successful use of robots in rehabilitation [1] and assistance [2] making the operating modes of the robotic system more flexible and compatible with the human subject [3], [4]. The benefits of reproducing the patient's personal motion style during robot-aided rehabilitation sessions are not well-established in literature yet, but the adoption of such an approach in traditional rehabilitation treatments demonstrated encouraging results. Take for example the mirror therapy in stroke. It requires to perform the movements of the non-paretic limb while viewing its mirror reflection superimposed over the unseen paretic limb [5]. This therapy helps prevent or reduce the learned non-use of the paretic limb and also enhance neuroplasticity, making the user to relearn his/her personal motion style [6].

A typical approach used to plan the motion of assistive and rehabilitation robots in a way similar to humans in the point-to-point motion is the minimum-jerk [7]. However, it cannot reproduce the subject's personal motion style. Approaches that can face such a problem are grounded on replicated movements [8], [9]. They use spline decomposition [10] or optimization of ad hoc developed objective functions [11], [12] for replicating on the robotic system the trajectories executed by the subject. Their main drawback is that they cannot manage environment variability and external perturbations.

A new approach to movement planning and imitation learning is represented by Learning by Demonstration (LbD), where the human subject is observed during the task execution and the robotic systems replicate the learned movement. LbD approaches, compared to a minimum jerk trajectory planner, have the possibility to easily replicate human-like movements (i.e. the subject's personal motion style) and more complex tasks. Moreover, compared to a simple replicator of a recorded trajectory, or to a spline-based fitting method, they offer the advantage to be adaptable to the environment variability and modify the initial and the final points of the demonstrated trajectory by keeping the same movement shape.

An example of LbD approach is the one based on a set of nonlinear differential equations, namely Dynamic Movement Primitives (DMPs), with a well-defined landscape attractor [13]. This attractor allows replicating the recorded trajectory by means of a weighted sum of equally spaced Gaussian Kernels; weight parameters (DMP parameters) are extracted from demonstrated movements, in a single shot, with a Locally Weighted Regression (LWR) algorithm.

In [14] it is shown that DMP overcomes performance of other LbD approaches. In particular, the comparison with the Time-dependent Gaussian mixture regression [15], the LWR [16] and

the locally weighted projection regression [18] demonstrated the advantages in terms of robustness to spatial perturbations, accuracy and computation time used by the learning process.

Therefore, LbD approach based on DMP seems to be very suitable for planning ADL movements in assistive robotics and robot-aided rehabilitation. ADL variability, due to the amount of motion tasks, environmental and context changes and variability of subjects' anthropometry, could require continuous robot motion re-planning for performing new specific tasks. LbD robot planning can face such a variability by replicating the human motion. Furthermore, rehabilitation and assistive robotics are involved in contexts e.g. domestic environment or rehabilitation center, where the simplicity of LbD-based motion planning could allow an operator without technical expertise, i.e. a therapist or a caregiver, to easily reproduce a new therapeutic exercise on the robot or to demonstrate the robot how to perform a new task at home [19].

Thus, the main objective of this work is to resort to the LbD method based on DMP and proposed in [13] for improving motion planning strategies in rehabilitation and assistive robotics. The overall idea is to develop a motion planning system that i) can be easily trained by human subjects who have not technical skills to program the robot in performing daily living tasks, ii) can replicate patient's personal motion style and iii) can be adaptable to the environment change. The developed system stores in a database a set of distinctive features of the trajectories recorded during demonstration. Subsequently, depending on the type of task and the target position, the system selects the proper set of features from the database and builds the trajectory to suitably accomplish the task. The proposed motion planning system is also able to manage modification in the robot initial and target pose as well as complex trajectories.

In this letter, a variation of LbD method presented in [13] is proposed. It is aimed to improve the accuracy of the trajectory reconstruction, thus allowing a better reproduction of the user's personal motion style, and to optimize the size of the database to be stored, thus achieving significant savings in terms of computational time to access the database. Due to the several amount of ADLs to be learned, the database size could reach high dimensions in daily living scenarios [17].

To this purpose, 1) an optimized kernel allocation depending on the trajectory complexity has been proposed. This complexity is mainly increased by critical points, such as minimum, maximum or inflection points, that are typical in complex trajectories such as the ones performed in ADLs. 2) The number of kernel is not a priori defined but it is properly found by means of a recursive method.

In particular, one can notice from [13] that the points of the trajectory worst approximated by LbD algorithm are the above mentioned critical points. In [13], in order to reduce the error in the trajectory reconstruction, an increase of the kernel functions number and, thus, of the DMP parameters number, is required. This could cause a significant extension of the memory size required to record the database in a scenario in which the amount of tasks to be learned by the robot could be high, requiring consequently a long processing time to access the database.

Therefore, an optimization of the number of DMP parameters required to ensure a reconstruction error less than a pre-set threshold is applied in this work. The optimization has been achieved by increasing the spatial distribution of the gaussian kernel in correspondence of the critical points of the trajectory. It will achieve significant savings in terms of size of the dataset to be recorded and of processing time to access the database.

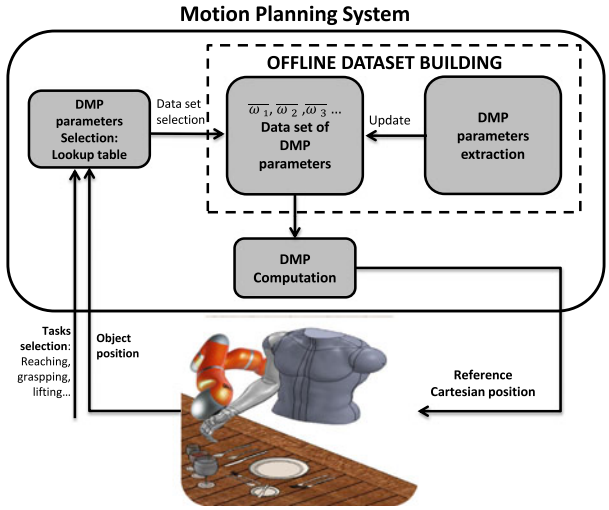

Fig. 1. Block scheme of the proposed motion planning system.

The proposed approach has been implemented and tested on the anthropomorphic robotic arm Kuka LWR 4+, and compared with the algorithm in [13] in order to assess its accuracy. Additionally, given the experimental scenario of robotic assistance during ADL execution, the generalization level of the proposed system is verified over 3 ADLs (i.e. drinking, eating and pouring), by evaluating the success rate of the task execution.

II. Methods

A. LbD Motion Planning System

The proposed Motion Planning System for rehabilitation and assistive robotics is shown in Fig. 1. Human motion trajectories are firstly recorded during the execution of ADLs. They are performed by a therapist, a caregiver or the patient itself with the sound arm and, as for typical LbD approaches, distinctive features (called DMP parameters) are subsequently extracted using a Locally Weight Regression algorithm. Hence, a dataset of DMP parameters is built (Off-line dataset building).

Afterwards, when a human subject (e.g. the patient) wants to perform one of the recorded ADLs with the robot assistance, an online extraction of the trajectory from the dataset is performed (DMP parameters selection). It consists of a lookup table, which selects the proper set of DMP parameters from the dataset, depending on the tasks type and objects position, and the algorithm for computing the DMP that best fit the desired task (DMP computation). In the following, theoretical details about the modules of DMP computation and DMP parameters extraction are provided.

B. DMP Computation

The DMP computation is grounded on a non-linear second order system, expressed as follows

$$\tau \ddot{y} = \alpha_y \left(\beta_y \left(g - y \right) - \dot{y} \right) + f \tag{1}$$

τ is a time constant, α_y and β_y are positive constants, y_0 and g are the initial and final point of the trajectory, respectively,

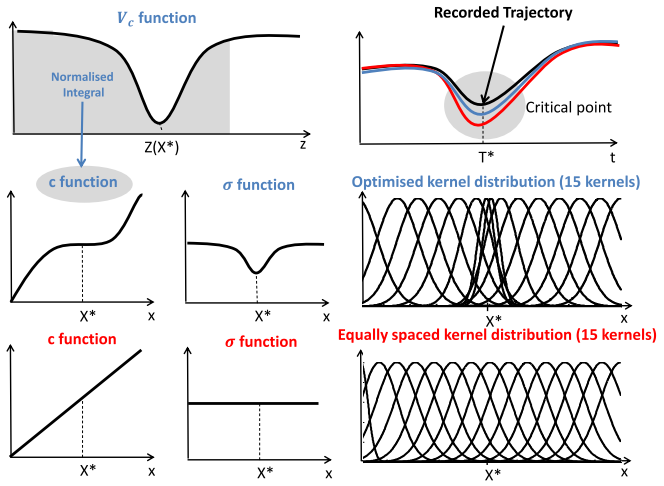

Fig. 2. c and σ function in the two different modality to allocate the Gaussian Kernels. The trajectories computed with equally spaced and optimised kernel distribution are outlined in red and blue, respectively. X* and T* are the state and time corresponding to the critical point.

and f is a forcing term that implements the landscape attractor of the system. The solution of equation (1), i.e. y, provides the trajectory named Dynamical Movement Primitive (DMP). In the following a set of 7 DMPs, $y_{J_1}, y_{J_2} ... y_{J_7}$, has been used as reference joint angles of the robot; moreover a set of 6 DMPs, $y_{C_1}, y_{C_2} \dots y_{C_6}$, has been used as reference Cartesian position. The corresponding derivatives, $\dot{y}_{J_1}, \dot{y}_{J_2} \dots \dot{y}_{J_7}$ and $\dot{y}_{C_1}, \dot{y}_{C_2} \dots \dot{y}_{C_6}$, are the joint and Cartesian velocity, respectively. As well, $\ddot{y}_{J_1}, \ddot{y}_{J_2} \dots \ddot{y}_{J_7}$ and $\ddot{y}_{C_1}, \ddot{y}_{C_2} \dots \ddot{y}_{C_6}$ are the joint and Cartesian acceleration, respectively. The forcing term is expressed as

$$f(x) = \frac{\sum_{i=1}^{N} \Psi_i(x)\,\omega_i}{\sum_{i=1}^{N} \Psi_i(x)} x\,(g - y_0) \tag{2}$$

In equation (2), $\Psi_i(x)$ are fixed basic functions written as Gaussian functions as

$$\Psi_i(x) = \exp\left(-\frac{1}{2\sigma^2}(x - c_i)^2\right) \tag{3}$$

where σ_i, c_i, N represent width, centres and number of Gaussian functions, ω_i are the weight parameters (i.e. the DMP parameters) used to fit the recorded trajectory, and x is a state variable introduced to delete the time dependency of the system. Indeed, it is worth noticing that time dependency of equation (1) is expressed as

$$\tau \dot{x} = -\alpha_x x \tag{4}$$

that relates time and state x of the whole system. In [13] the range of variation of state x and centres c_i is [0, 1] and c_i is a monotonic linear function of x (bottom left in Fig. 2); hence, the Gaussian kernels are equally distributed over x. In the approach proposed in this letter, the spatial distribution of the Gaussian kernels is varied in order to increase the kernel number in the critical points, by keeping constant the total number of kernel functions for a given trajectory (in the joint space as well as in the full task space), and consequently reduce the error between the human recorded trajectory and the robot learned one. To this purpose, c_i and σ_i are defined as follows

$$c(x) = \frac{\int_0^x V_c(z)\,dz}{||\int_0^1 V_c(z)\,dz||} \tag{5}$$

$$V_c(z) = 1 - \alpha_z \sum_{k=1}^{p} \exp\left(-\beta_z\,(z - z_k)\right) \tag{6}$$

$$\sigma(x) = \gamma_z \frac{V_c(x)}{N} + \delta_z \tag{7}$$

$$c_i = c\left(\frac{i}{N}\right) \tag{8}$$

$$\sigma_i = \sigma\left(\frac{i}{N}\right) \tag{9}$$

where $\alpha_z, \beta_z, \gamma_z$ and δ_z are positive constants, P is the number of critical points of the recorded trajectory and z_k is the normalised time instant of these critical points. In Fig. 2 an example of c and σ function for both the different modality to allocate the Gaussian Kernels is provided.

C. DMP Parameters Extraction

A locally weighted regression (LWR) algorithm [16] is adopted to learn DMP parameters ω_i in equation (2). Data $y_d, \dot{y}_d$ and $\ddot{y}_d$, i.e. position, velocity and acceleration, from the recorded trajectories (joint angles or Cartesian positions) are inserted in the forcing term of equation (2) as follows

$$f_t = \tau^2 \ddot{y}_d - \alpha_y\left(\beta_y\,(g - y_d) - \tau \dot{y}_d\right) \tag{10}$$

hence, a function approximation problem is formulated in order to find ω_i parameters that make f_t as closed as possible to f. For each kernel function $\Psi_i(t)$, LWR looks for the corresponding ω_i that minimises the locally weighted quadratic error through the following cost function

$$J_i = \sum_{t=1}^{P} \Psi_i(t)\,(f_t(t) - \omega_i \epsilon(t))^2 \tag{11}$$

$$\epsilon(t) = x\,(g - y_0) \tag{12}$$

III. Experimental Protocol

A. Experimental Setup

The motion planning system in Fig. 1 has been tested on an anthropomorphic robotic arm (i.e. the KUKA-LWR 4+) in an experimental scenario of assistance to a human subject during the execution of ADLs (Fig. 3). The KUKA-LWR 4+ is a 7 DoFs anthropomorphic robotic arm with position and torque sensors at joints. The communication between the robot and a remote PC is guaranteed by the Fast Research Interface (FRI) Library, which runs on a remote PC connected to the KUKA Robot Controller via a UDP communication protocol. Eight healthy subjects volunteered to participate in the experimental validation. They have been asked to perform three ADLs (i.e. drinking, eating and pouring), with the wrist attached to the robot end-effector by means of a purposely developed flange. Each ADL has been divided into a number of subtasks listed in the following:

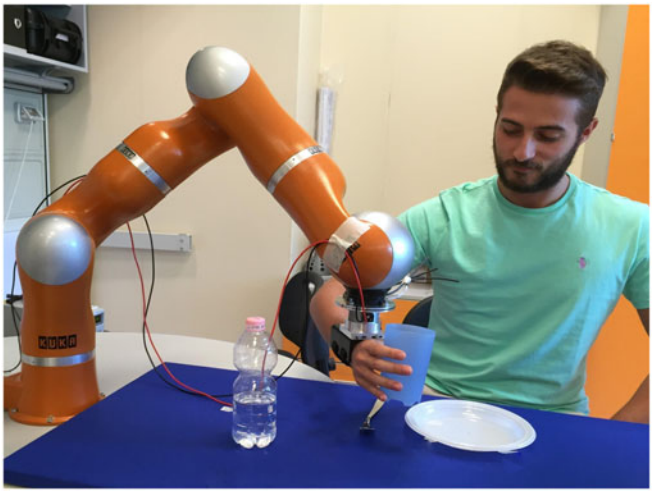

Fig. 3. Experimental setup.

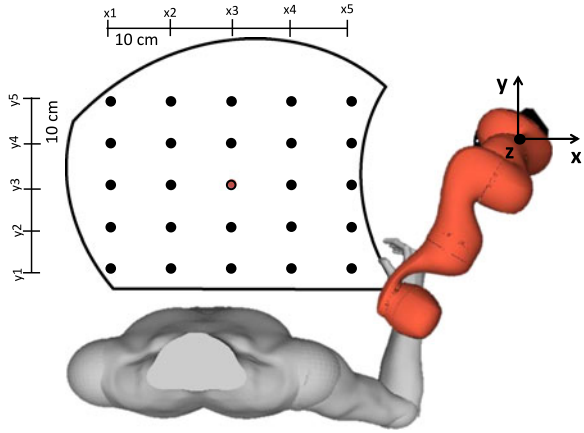

Fig. 4. Human-robot workspace (delimited by the black line). The positions in which the objects are moved in the considered workspace with respect to a initial recording position (red dot) are outlined with black dots.

1) The drinking task has been divided into 4 subtasks: reach the glass, reach the mouth, reach the table for releasing the glass, go back to the rest position;
2) The eating task has been divided into 5 subtasks: reach the cutlery, reach the dish, take the food and reach the mouth, reach the table for releasing the cutlery, go back to the rest position;
3) The pouring task has been divided into 4 subtasks: reach the bottle, pour the water, release the bottle, go back to the rest position.

The experimental validation consisted of two different sessions, described below. Each session could be divided into two phases: a) DMP parameters extraction and b) DMP computation.

1) 1st Experimental Session: The first experimental session aimed at comparing the proposed version of DMP computation module in Eqs. (5)–(8) with respect to the original formulation in [13]. The main difference is in the allocation of Gaussian kernels and the main findings are related to the trajectory reconstruction error, the reproduction accuracy of the user's personal motion style and the required memory allocation for the database of DMP parameters.

a) DMP parameters extraction: In the 1st phase, the robotic arm worked in a passive mode: the subject's arm actively guided the robot arm by the wrist, and robot sensors have been used to record joint trajectories. Cartesian trajectories have been subsequently computed via forward kinematics. Each task has been repeated five times. The subject was seated in front of a table where the objects were placed in a priori known position. Each trial started from the same initial configuration in which the shoulder was abducted of 0° in the frontal plane and flexed with an angle of 0° in the sagittal plane, the elbow was flexed with an angle of 90° in the sagittal plane and the wrist was in a neutral position with 0^o for flexion/extension, 0° for radio-ulnar deviation and 0° for prono/supination. Subsequently, DMP parameters has been extracted from the 7 joint trajectories and the 6 cartesian position for each task and trial.

b) DMP computation: In the second phase the robot arm worked in an active mode. Firstly, DMPs have been computed in the joint space. The subject arm has not been attached to the robot end-effector and DMPs have been replicated by means of a PID position control with the purpose of measuring performance of the two algorithms in the case of highest level of robot accuracy (0.002 rad). Subsequently, DMPs have been computed in the Cartesian space. The subject arm has been attached to the robot and has been passively guided in the execution of the 3 ADLs with an impedance control with high gains (for the position variables gains were set to 2000 N/m for stiffness and 0.7 N·s/m for damping; for the orientation variables the gains were set to 2000 N·m/rad for stiffness and 0.7 N·m·s/rad for damping). This setting makes the robot provide the patient with a high level of assistance. The two algorithms have been compared in terms of reconstruction error between the recorded and the DMP trajectory, given the same number of Gaussian kernels, and number of DMP parameters for ensuring a trajectory reconstruction error lower than a preset threshold (5% of $\|g - y_0\|$, where y_0 and g are the initial and final point of the trajectory). This threshold corresponds to a reconstruction error of 0.02 m calculated on a maximum Cartesian motion of 0.4 m (see Fig. 4) and of 0.08 rad calculated on a maximum orientation angle of 1.57 rad. This value is especially significant during the execution of activities of daily living that require high motion accuracy. Take, for example, opening/closing a drawer, a window, a door, a jar and other activities that require to strictly track motion for a successful result.

Additionally, measures of the algorithm capability to accurately reproduce the user's personal motion style and of the memory allocation required to record DMP parameters in a database have been carried out.

2) 2nd Experimental Session: The 2nd experimental session aimed to demonstrate the algorithm capability to generalize with respect to the object position changes. To this purpose, the target objects used in the ADLs (i.e. glass for drinking, bottle for pouring and plate for eating) have been placed in 24 different positions of the human-robot workspace, with respect to initial recording position (i.e. the point of coordinates $[X_3, Y_3]$ in Fig. 4. The glass to be filled during pouring task and the fork to be used during eating task have not been moved from

the initial position, i.e. $[-0.04, -0.41]$ m and $[-0.6, -0.34]$ m, respectively, in the robot reference frame.

a) DMP parameters extraction: The first phase of the 2nd session is similar to the one of the 1st session. The subject's arm actively moved the robot by the wrist during the execution of the 3 ADLs. The task has been repeated for 5 times. Joint angles have been recorded by the sensors embedded in the robotic arm and Cartesian trajectories have been computed via forward kinematics. Subsequently, DMP parameters have been extracted from the mean of 5 trials computed on the 6 Cartesian positions for each sub-task.

b) DMP computation: In the 2nd phase, DMPs have been computed in the Cartesian space (6 DMPs for each sub-task and object position). The subject's wrist has been assisted by the robotic arm to perform the previously described ADLs with an impedance control with high gains, thus achieving a high level of assistance. For the position variables gains were set to 2000 N/m for stiffness and 0.7 N·s/m for damping; for the orientation variables the gains were taken as 2000 N·m/rad for stiffness and 0.7 N·m·s/rad for damping. The algorithm capability to generalize with respect to the change in the object position has been measured through the task execution success rate.

B. Data Analysis

Recorded joint trajectories and Cartesian positions have been processed with a digital 1st order Low Pass Filter with a cut-off frequency of 20 Hz and subsequently segmented. For segmentation, the time instants when the velocity grows up or decreases to the 10% of the peak value have been considered.

For the 1st experimental session a set of DMP parameters has been extracted with a preset number of 30 Gaussian Kernels, on the 5 trials of each sub-task per subject. DMP computation for the 7 joints and 6 Cartesian positions is then applied with the two versions of spatial allocation of the Gaussian kernels. They have been compared, on real hardware, in terms of Normalised Displacement Error (NDE) expressed as

$$NDE = \frac{DE}{\|g - y_0\|} 100 \tag{13}$$

where DE is the displacement error between recorded trajectories and the learned ones in output from the algorithms. It is worth noticing that the amplitude of the displacement error depends on the trajectory Range of Motion (RoM). Subsequently, a recursive algorithm has been performed in order to find the proper number of DMP parameters required to ensure a threshold NDE of 5% on all the trajectories adopting the two versions of spatial allocation of the Gaussian kernels and two proper databases, one for each version, have been built.

Database Memory Size (MS) has been expressed as

$$MS = \sum_{i=1}^{T} \sum_{j=1}^{7} 4N_{ij}, \quad \text{[byte]} \tag{14}$$

where T is the total number of sub-tasks and N_{ij} is the number of parameters required for fitting the ij-th trajectory. In equation (14) we suppose to store floating point of 4 bytes.

In order to compute the time required to scroll the two databases, and thus the time to select the queue set of parameters in the stored databases, a time index has been introduced. It refers to the computational complexity needed to perform a linear search in the two databases. It is expressed as

$$T_{ind} = \frac{o(N_a)}{o(N_b)} \tag{15}$$

where T_{ind} is the proportional factor between the time required to scroll the two databases and N_a and N_b are the number of parameters stored in them. $o(.)$ symbolically express the asymptotic behavior of N_a and N_b. Algorithm capability to accurately reproduce the user's personal motion style is measured through a motion style index expressed as

$$MSI = \sqrt{\frac{1}{N} \sum_{J=0}^{N} \left(a_{ij}^r - a_{ij}^c\right)^2} \tag{16}$$

where N is the number of time instants, a_{ij}^r is the acceleration of the i-th recorded Cartesian position at the j-th time instant and a_{ij}^c is the acceleration of the i-th Cartesian position computed at the j-th time instant by means of the DMP algorithm.

In the 2nd experimental session, mean value and Standard Deviation (SD) of the segmented Cartesian trajectories have been computed on the 5 trials of each sub-task per subject, and a set of DMP parameters has been extracted by adopting our proposed algorithm in order to build a database. The recorded parameters have been used to compute the Cartesian DMPs by means of the DMP computation algorithm, for each sub-task and for different initial and final positions. Given the high robot repeatability, i.e. ± 0.05 mm, the tasks have been executed one time per object position. System generalization capabilities have been evaluated in terms of the success rate of the task execution.

Mean value and SD of the all previously described indices have been computed on the eight subjects. Hence, a statistical analysis based on Wilcoxon paired-sample test has been performed. Since this analysis has been carried out on multiple comparisons, the significant factor has been corrected with Bonferroni method. Therefore, it has been reported for $p{-}value < 0.05/n_c$, where n_c is the number of multiple comparisons.

IV. Results

A. 1st Session Experimental Results

Figs. 5(a) and 6(b) report two representative joint trajectories of one subtask (i.e. reaching the cutlery). In particular, the trajectories of joints 3 and 5 executed by a representative subject are reported, but similar trajectories are executed for the other joints and by the other subjects. These figures show how well the optimized kernel distribution and equally spaced kernels perform the recorded trajectory approximation in two types of critical points, i.e. inflection [Fig. 5(a)] and minimum [Fig. 6(a)] points. Figs. 5(b) and 6(b) report, for joint 3 and 5 respectively, the error of the recorded trajectory approximation, when the optimized kernel distribution and equally spaced kernels are adopted. This error is normalized with respect to the recorded trajectory RoM. The time is normalized, as well, with respect to the time needed to complete the movement (t_f). From Figs. 5(b) and 6(b) it is evident that a better approximation of the recorded trajectory is achieved in the critical points when the kernel distribution is optimized.

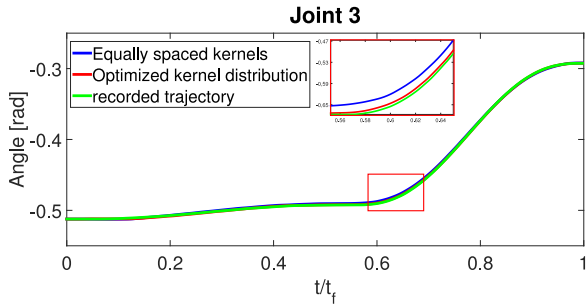

(a)

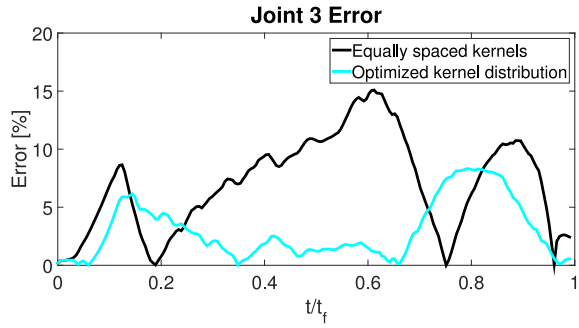

(b)

Fig. 5. Joint 3: (a) trajectory and (b) reconstruction error computed for a representative subject.

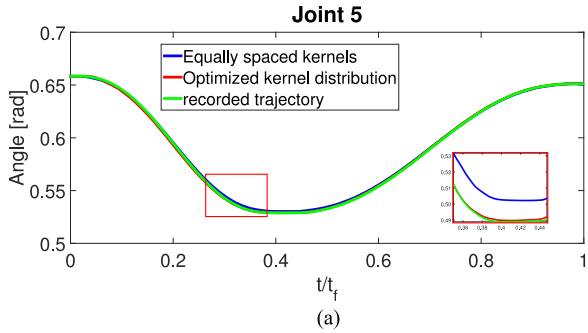

(a)

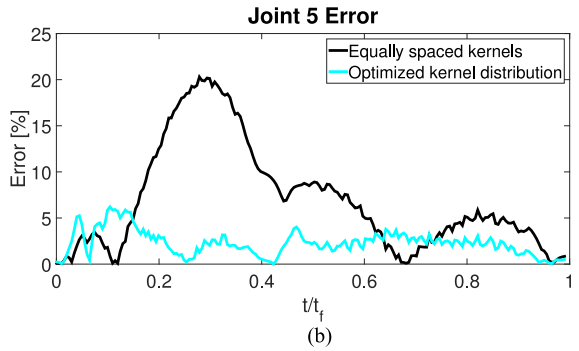

(b)

Fig. 6. Joint 5: (a) trajectory and (b) reconstruction error computed for a representative subject.

Furthermore, in Tables I and II the NDE of the joint angles and Cartesian positions, with mean value and SD is reported. It has been computed on each task and subject for both the versions of kernel distribution.

TABLE I
JOINT NDE % OBTAINED IN SESSION I

Equally spaced kernels[1]							
Task	Joint 1	Joint 2	Joint 3	Joint 4	Joint 5	Joint 6	Joint 7
1	15 ± 6	20 ± 4	25 ± 5	19 ± 3	15 ± 6	21 ± 6	22 ± 3
2	12 ± 4	19 ± 10	16 ± 4	18 ± 2	16 ± 4	25 ± 5	18 ± 4
3	16 ± 5	21 ± 6	17 ± 3	14 ± 5	23 ± 3	18 ± 10	19 ± 11
Optimized kernel distribution[1]							
Task	Joint 1	Joint 2	Joint 3	Joint 4	Joint 5	Joint 6	Joint 7
1	4 ± 3	7 ± 2	6 ± 3	5 ± 2	5 ± 5	6 ± 4	7 ± 3
2	6 ± 4	4 ± 6	7 ± 3	3 ± 1	4 ± 3	7 ± 4	3 ± 2
3	3 ± 1	2 ± 2	7 ± 2	4 ± 3	8 ± 3	4 ± 5	5 ± 4

[1]These results were achieved piloting the robot with PID control.

TABLE II
CARTESIAN NDE % OBTAINED IN SESSION I

Equally spaced kernels[2]							
Task	X	Y	Z	Q_0	Q_1	Q_2	Q_3
1	22 ± 6	25 ± 6	23 ± 6	24 ± 8	19 ± 7	25 ± 9	21 ± 6
2	24 ± 5	21 ± 5	20 ± 7	25 ± 5	22 ± 6	23 ± 6	27 ± 8
3	19 ± 7	18 ± 7	18 ± 5	20 ± 5	24 ± 3	21 ± 5	26 ± 9
Optimized kernel distribution[2]							
Task	X	Y	Z	Q_0	Q_1	Q_2	Q_3
1	7 ± 6	7 ± 5	3 ± 4	7 ± 5	5 ± 5	4 ± 3	5 ± 2
2	9 ± 8	5 ± 6	9 ± 7	8 ± 4	6 ± 2	4 ± 5	7 ± 4
3	6 ± 9	4 ± 6	8 ± 5	13 ± 2	3 ± 4	3 ± 4	8 ± 3

[2]These results were achieved piloting the robot with an impedance control.

On one hand, it could be noticed that the optimized kernel distribution provides an average improvement of the NDE for the 7 joint angles of 15%, 13% and 14% for task 1, 2 and 3, respectively. This corresponds to an average improvement of 0.10 rad, 0.091 rad and 0.098 rad, respectively, if computed on the average motion of the performed joint trajectories, i.e. $\|g - y_0\|$.

On the other hand, for task 1, 2 and 3, an average improvement of the NDE in the 3 Cartesian positions of 17%, 14% and 12% is observed; while for the 4 quaternion parameters an average improvement of 17%, 18% and 16% is observed for each task. These values correspond to a Cartesian position error of 0.034 m, 0.028 m and 0.024 m and to an orientation error (expressed in unit quaternion) of 0.020, 0.021 and 0.019 for task 1, 2 and 3, respectively, if computed on the average motion of the performed trajectories, i.e. $\|g - y_0\|$. It is worth noticing that such an error reduction is especially substantial for the execution of activities of daily living that require high motion accuracy along the trajectory, such as opening/closing a drawer, a window, a door, a jar and other tasks that require to strictly track a motion. Indeed, an error of a few centimeters (about 0.02 m) and a few degrees (about 0.012 in quaternion representation and about 4.5° in Euler Angles representation) could compromise their accomplishment. The benefit due to the improvement of position and orientation NDE can further grow if the approach is extended to the control of robotic devices for hand rehabilitation and assistance, which could require significantly higher motion accuracy.

TABLE III
NUMBER OF KERNELS (N_G) OBTAINED IN SESSION I

Equally spaced kernels[2]							
Task	X	Y	Z	Q_0	Q_1	Q_2	Q_3
1	208 ± 14	255 ± 21	220 ± 24	250 ± 21	145 ± 16	220 ± 15	242 ± 20
2	237 ± 16	188 ± 22	170 ± 12	360 ± 23	340 ± 18	203 ± 14	156 ± 15
3	210 ± 17	350 ± 18	230 ± 18	270 ± 16	254 ± 19	313 ± 21	201 ± 18
Optimized kernel distribution[2]							
Task	X	Y	Z	Q_0	Q_1	Q_2	Q_3
1	92 ± 10	91 ± 16	55 ± 14	100 ± 8	65 ± 15	71 ± 10	66 ± 11
2	124 ± 11	70 ± 15	123 ± 11	115 ± 7	90 ± 16	82 ± 13	98 ± 9
3	130 ± 12	95 ± 11	170 ± 17	95 ± 14	85 ± 13	63 ± 14	72 ± 15

[2]These results were achieved piloting the robot with an impedance control.

TABLE IV
MOTION STYLE INDEX (MSI) OBTAINED IN SESSION I

Equally spaced kernels[2]							
Task	X[3]	Y[3]	Z[3]	Q_0[4]	Q_1[4]	Q_2[4]	Q_3[4]
1	7 ± 0.6	6 ± 0.5	0.7 ± 0.6	9 ± 0.9	8 ± 2	7 ± 3	9 ± 4
2	6 ± 1	9 ± 0.6	13 ± 0.5	11 ± 1	10 ± 0.7	12 ± 3	13 ± 3
3	8 ± 0.9	7 ± 0.8	11 ± 0.7	8 ± 3	12 ± 4	13 ± 1	11 ± 4
Optimized kernel distribution[2]							
Task	X[3]	Y[3]	Z[3]	Q_0[4]	Q_1[4]	Q_2[4]	Q_3[4]
1	3 ± 0.1	2 ± 0.2	0.3 ± 0.3	3 ± 0.3	1 ± 0.3	2.3 ± 0.3	1.2 ± 0.2
2	1 ± 0.1	0.9 ± 0.1	0.5 ± 0.1	2 ± 0.2	0.7 ± 0.2	1.2 ± 0.2	2.3 ± 0.1
3	2 ± 0.3	0.8 ± 0.2	0.7 ± 0.2	4 ± 0.4	0.5 ± 0.4	0.5 ± 0.3	0.8 ± 0.5

[2]These results were achieved piloting the robot with an impedance control.
[3]The units of these values are $[\mathrm{cm/s^2}]$.
[4]The units of these values are $[10^{-3}/\mathrm{s^2}]$.

The statistical analysis performed with a Wilcoxon paired-sample test over eight subjects and 5 trials, for each task, showed significant differences in the joint space ($p\text{-}value < 0.016$ over the 7 joint angles in Table I for each task), and in the Cartesian space ($p\text{-}value < 0.0083$ over the 3 Cartesian coordinates for task 1 and 2 and over the 4 quaternion parameters in Table II for each task).

Additionally, in Table III the mean value and SD of the number of DMPs (N_G) required to reach a NDE lower than 5% are reported, for all the Cartesian positions. They are computed over the eight subjects, for each task, for the both versions of Gaussian distribution. Significant differences between the two different modalities of allocation of Gaussian kernels have been achieved. Again, the statistical analysis was performed through the Wilcoxon paired-sample test over eight subjects and 3 Cartesian position for each task, and over eight subjects and 4 quaternion parameters for each task.

Two databases (named database1 and database2) have been built for the optimized kernel distribution and the equally spaced kernels, respectively. The mean value and SD of the memory size occupied by the two databases have been computed over the eight subjects. Database1 has a size of 4.5 ± 0.7 MB, while database2 has a size of 7.3 ± 0.9 MB. Hence, 2.8 ± 0.9 MB have been saved with the optimized kernel distribution. Moreover, considerations about the computational saving could be extracted by replacing in Eq. (15) the values in Table III. A time index (T_{ind}) equal to 0.61 has been obtained, indicating that the time to scroll database2 is about 61% of the time to scroll database1.

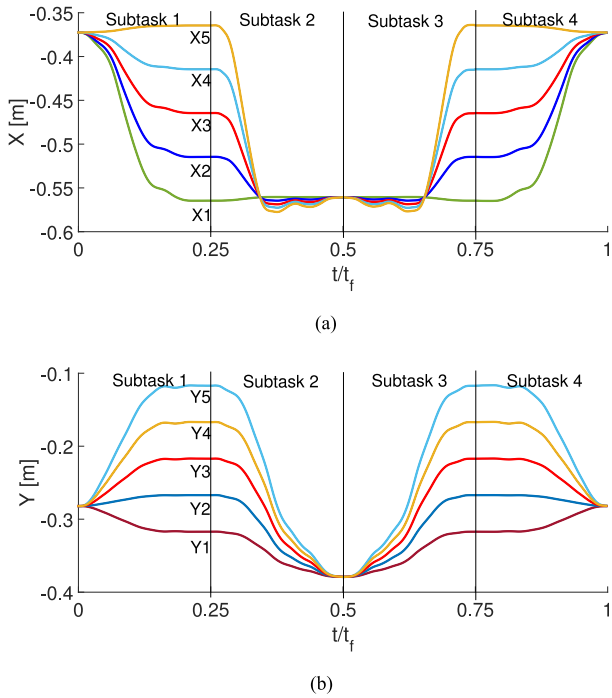

Fig. 7. Cartesian coordinate trajectories executed by the robotic arm during the drinking task with 24 glass different positions. (a) X coordinate. (b) Y coordinate. The recorded trajectory is outlined in red.

Time and memory savings are directly proportional to the number of stored parameters. Hence, saving could significantly increase if the number of tasks grows. For instance, in a home scenario there could be hundreds of possible tasks involving interaction with the environment [17]; thus, a memory saving of hundreds of MB, with a correspondent time saving of some seconds, can be achieved. In a rehabilitation scenario where the amount of patients treated per year is significantly higher, the above mentioned savings could be notably increased.

Finally, in Table IV the mean value and SD of the motion style index, calculated over the eight subjects for the two versions of spatial allocation of the Gaussian kernels, are reported. Accuracy increase is achieved in the user's personal motion style reproduction when the optimised kernel distribution is adopted. The motion style index is reduced by about $2\,\mathrm{cm/s^2}$, $8\,\mathrm{cm/s^2}$ and $7\,\mathrm{cm/s^2}$ on average of the 3 Cartesian axes and is reduced of about $6\,10^{-3}/\mathrm{s^2}$, $9\,10^{-3}/\mathrm{s^2}$ and $10\,10^{-3}/\mathrm{s^2}$ on average of the 4 quaternion parameters, for task 1, 2 and 3, respectively. It is interesting to note that the improvements achieved in terms of user motion style reproduction are statistically significant, as verified with the Wilcoxon paired-sample test on 5 trials and eight subjects, applied both to the 3 Cartesian axes and to the 4 quaternion parameters for each task ($p\text{-}value < 0.0083$).

B. 2nd Session Experimental Results

X and Y Cartesian trajectories, executed by the robotic arm in assisting a representative subject to perform drinking and eating task, are shown in Figs. 7 and 8. The other Cartesian coordinates are not shown, being Z and orientation coordinates not varied when the objects are placed in the 24 different positions of Fig. 4.

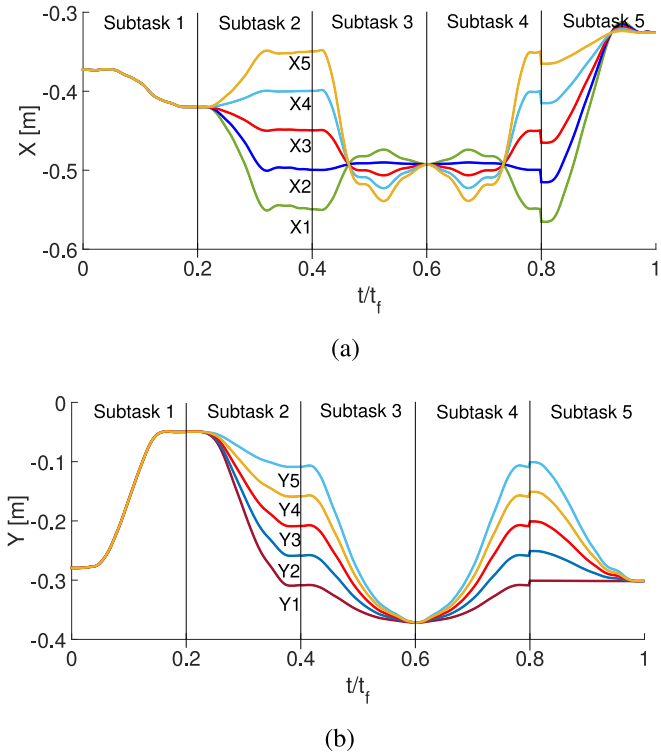

Fig. 8. Cartesian coordinate trajectories executed by the robotic arm during the eating task with 24 plate different positions. (a) X coordinate. (b) Y coordinate. The recorded trajectory is outlined in red.

Furthermore, also pouring task is not shown being very similar to the drinking task in terms of X and Y Cartesian trajectories. In Fig. 7 and 8 the red trajectory refers to the recorded one (in this case objects are in $[X_3, Y_3]$ position). It could be noticed from these figures that the different target positions of the object, i.e. $[X_1, Y_1], [X_1, Y_2] \ldots [X_4, Y_5], [X_5, Y_5]$ of Fig. 4, are reached with a movement shape similar to the recorded one in all the tasks. Similar results have been achieved over the other subjects. In summary, a success rate of 100% for all the tasks has been achieved on the eight subjects.

V. Conclusion

In this work a Motion Planning System for rehabilitation and assistive robotics, grounded on LbD approach, has been proposed. The LbD algorithm presented in this work is grounded on DMPs as in [13], but it is improved by introducing an optimized kernel allocation depending on the trajectory complexity. In particular, the spatial distribution of the gaussian kernels (the number of which is properly found by means of a recursive method), used to fit the recorded trajectory, is increased in correspondence of the critical points in order to reduce the number of DMP parameters required to ensure a reconstruction error less than a pre-set threshold. This change allowed us achieving significant savings in terms of size of the database to be recorded, being equal the accuracy in the reproduction of user personal motion style. It is particularly important in daily living scenarios where several amount of ADLs should be learned. Future efforts will be mainly addressed to automate the dataset access by providing the system, in real time, with information about the environment (e.g. the object position and interaction forces [20]) and the user's intention (i.e. the type of task to be accomplished). Furthermore, an extensive experimental validation will be carried out on patients to investigate and quantify the benefits of the proposed approach in clinical settings and on further examples of human robot interaction tasks.

References

[1] F. Amirabdollahian, R. Loureiro, and W. Harwin, "Minimum jerk trajectory control for rehabilitation and haptic applications," in *Proc. IEEE Int. Conf. Robot. Autom.*, 2002, vol. 4, pp. 3380–3385.
[2] K. Dautenhahn, S. Woods, C. Kaouri, M. L. Walters, K. L. Koay, and I. Werry, "What is a robot companion-friend, assistant or butler?" in *Proc. IEEE/RSJ Int. Conf. Intell. Robots Syst.*, 2005, pp. 1192–1197.
[3] L. Zollo, A. De Luca, and B. Siciliano, "Regulation with on-line gravity compensation for robots with elastic joints," in *Proc. IEEE Int. Conf. Robot. Autom.*, 2004, vol. 3, pp. 2687–2692.
[4] D. Accoto, G. Carpino, F. Sergi, N. L. Tagliamonte, L. Zollo, and E. Guglielmelli, "Design and characterization of a novel high-power series elastic actuator for a lower limb robotic orthosis," *Int. J. Adv. Robot. Syst.*, vol. 10, no. 359, pp. 1–12, 2013.
[5] S. Stbeyaz, G. Yavuzer, N. Sezer, and B. F. Koseoglu, "Mirror therapy enhances lower-extremity motor recovery and motor functioning after stroke: A randomized controlled trial," *Arch. Phys. Med. Rehabil.*, vol. 88, pp. 555–559, 2007.
[6] C. Dohle, J. Pllen, A. Nakaten, J. Kst, C. Rietz, and H. Karbe, "Mirror therapy promotes recovery from severe hemiparesis: A randomized controlled trial," *Neurorehabil Neural Repair*, vol. 23, pp. 209–217, 2009.
[7] T. Flash and N. Hogan, "The coordination of arm movements: an experimentally confirmed mathematical model," *J. Neurosci.*, vol. 5, no. 7, pp. 1688–1703, 1985.
[8] C. H. An, C. G. Atkeson, and J. M. Hollerbach, *Model-Based Control of a Robot Manipulator*. Cambridge, MA, USA: MIT Press, 1988.
[9] F. Cordella, F. Di Corato, G. Loianno, B. Siciliano, and L. Zollo, "Robust pose estimation algorithm for wrist motion tracking," in *Proc. IEEE/RSJ Int. Conf. Intell. Robots Syst.*, 2013, pp. 3746–3751.
[10] J. Aleotti and S. Caselli, "Robust trajectory learning and approximation for robot programming by demonstration," *Robot. Auton. Syst.*, vol. 54, no. 5, pp. 409–413, 2006.
[11] A. Provenzale, F. Cordella, L. Zollo, A. Davalli, R. Sacchetti, and E. Guglielmelli, "A grasp synthesis algorithm based on postural synergies for an anthropomorphic arm-hand robotic system," in *Proc. IEEE Int. Conf. Biomed. Robot. Biomechatronics*, 2014, pp. 958–963.
[12] U. Pattacini, F. Nori, L. Natale, G. Metta, and G. Sandini, "An experimental evaluation of a novel minimum-jerk cartesian controller for humanoid robots," in *Proc. IEEE/RSJ Int. Conf. Intell. Robots Syst.*, 2010, pp. 1668–1674.
[13] A. J. Ijspeert, J. Nakanishi, H. Hoffmann, P. Pastor, and S. Schaal, "Dynamical movement primitives: Learning attractor models for motor behaviors," *Neural Comput.* vol. 25, no. 2, pp. 328–373, 2013.
[14] S. Calinon, F. D'halluin, E. Sauser, D. Caldwell, and A. Billard, "Learning and reproduction of gestures by imitation: An approach based on hidden Markov model and gaussian mixture regression," *IEEE Robot. Autom. Mag.*, vol. 17, no. 2, pp. 44–54, Jun. 2010.
[15] S. Calinon and A. Billard, "Statistical learning by imitation of competing constraints in joint space and task space," *Adv. Robot.*, vol. 23, no. 15, pp. 2059–2076, 2009.
[16] S. Schaal and C. Atkeson, "Constructive incremental learning from only local information," *Neural Comput.*, vol. 10, no. 8, pp. 2047–2084, 1998.
[17] D. Roggen *et al.*, "Collecting complex activity datasets in highly rich networked sensor environments," in *Proc. 7th Int. Conf. Netw. Sens. Syst.*, 2010, pp. 233–240.
[18] S. Vijayakumar, A. D'souza, and S. Schaal, "Incremental online learning in high dimensions," *Neural Comput.*, vol. 17, no. 12, pp. 2602–2634, 2005.
[19] C. G. Atkeson *et al.*, "Using humanoid robots to study human behaviour," *IEEE Intell. Syst.*, vol. 15, no. 4, pp. 46–56, Jul./Aug. 2000.
[20] P. Saccomandi, E. Schena, C. M. Oddo, L. Zollo, S. Silvestri, and E. Guglielmelli, "Microfabricated tactile sensors for biomedical applications: A review," *Biosensors*, vol. 4, no. 4, pp. 422–448, 2014.